Journal of Transport Geography 118 (2024) 103934

Contents lists available at ScienceDirect

Journal of Transport Geography

journal homepage: www.elsevier.com/locate/jtrangeo

Incorporating geographic interdependencies into the resilience assessment of multimodal public transport networks

Georgia Boura [*], Neil S. Ferguson

Department of Civil and Environmental Engineering, James Weir Building, University of Strathclyde, G1 1XJ Glasgow, UK

ARTICLE INFO

Keywords:
Redundancy
Substitutability
Resilience
Proximity
Geographic interdependency
Public transport

ABSTRACT

Severe weather events, such as snowfall, flooding and storms, may affect wide geographical areas and adversely impact discrete transport infrastructure networks (e.g. road, rail) at the same time, thus revealing the existence of geographic interdependencies between these networks. In this paper, we develop two accessibility-based measures to assess the impact of geographic interdependency on resilience based on the concepts of redundancy and substitutability, respectively. These measures are applied to the railway and long-distance bus networks in Scotland. Results reveal that the combined effect of redundancy and substitutability on the accessibility of locations offered by these discrete modes is reduced due to geographic interdependencies, with the extent of losses being positively associated with the spatial footprint of potential events. The results can be used to identify parts of the network where the potential impacts of geographic interdependencies are greatest, and thus require more in-depth scrutiny by network managers.

1. Introduction

The effective functioning of the public transport system is placed at risk by naturally-occurring, spatially-defined events such as earthquakes, rainfall, flooding and landslides. These events have the capacity to disrupt transport infrastructure and, in areas affected by such events, discrete transport networks carrying separate public transport modes (e.g. railway and bus) are at risk of concurrent disruption. For example, heavy snowfall in March 2018 caused widespread railway and road closures in Scotland affecting train and bus services (Network Rail, 2020). More recently, in July 2021, heavy and prolonged rainfall caused extensive flooding in central Germany and Belgium, leading to damage of railway lines, roads and bridges (Fathom Global, 2021). Human-caused climate change is expected to intensify and alter patterns of extreme weather around the world in the coming decades, including increases in heavy precipitation, flooding and heat, thereby increasing the risk of transport disruption (Lee et al., 2023).

Infrastructure networks which are located in close proximity to each other are said to be geographically (or spatially) interdependent if a hazardous event can disrupt both networks at the same time (Rinaldi et al., 2001; Zimmerman, 2004; Dudenhoeffer et al., 2006). As such, discrete public transport networks located in corridors defined by the natural landscape or built environment are particularly susceptible to concurrent disruption. From the public transport users' perspective, geographical interdependency reduces the added benefit of flexibility which exists when more than one transport mode is available.

The resilience of a transport system represents its ability to resist, absorb, adapt and quickly recover from the impact of hazardous events (Jenelius and Mattsson, 2020). Redundancy is a key component of transport system resilience (Bruneau et al., 2003) and in its simplest form is equal to the total number of (feasible) options, such as paths and transport modes, which exist between locations (Berdica, 2002). By weighting each option by a function of travel deterrence, a generalised measure of redundancy is obtained which is equivalent to established measures of accessibility (Ben-Akiva and Lerman, 1985; Anas, 1983; Xi et al., 2018). High levels of redundancy help maintain connectivity between locations in the event of disruption. However, it is also evident that spatially-defined events may reduce redundancy in geographically interdependent systems. Although a number of studies have considered the redundancy of single and multimodal networks with shared infrastructure (e.g. Frappier et al., 2018; Liao and van Wee, 2017), and whilst there is a growing body of research addressing geographical interdependencies between civil infrastructure systems (Patterson and Apostolakis, 2007; Johansson and Hassel, 2010; Pant et al., 2016; Thacker et al., 2017; Kays et al., 2023), to the authors' knowledge there has been no attention paid to the effect of geographical

* Corresponding author.
E-mail address: georgia.boura@strath.ac.uk (G. Boura).

https://doi.org/10.1016/j.jtrangeo.2024.103934
Received 13 November 2023; Received in revised form 27 June 2024; Accepted 1 July 2024
Available online 3 July 2024

interdependencies on the redundancy of discrete transport networks carrying separate public transport modes.

Recently the concept of substitutability was introduced into the literature (Van Wee et al., 2019). Substitutability is defined as the level of accessibility which is preserved in the event of the unavailability of a preferred option and reflects the capacity of the transport system to absorb the impact of disruptive events. As with redundancy, the level of substitutability will be reduced as a result of geographical interdependencies between public transport modes. A comparison of the concepts of redundancy and substitutability, with and without consideration of geographical interdependency, is given in Fig. 1. Whilst the attractiveness of preferred option (A) relative to the attractiveness of other options (B, C and D) does not affect the level of redundancy (or accessibility) offered by the set of options, it does affect the level of substitutability. Consequently, it is argued that both redundancy and substitutability can give important and complementary insights into public transport system resilience when considered within an accessibility framework.

Redundancy and substitutability are closely related to but distinct from the robustness of a transport system which reflects its capacity to withstand an adverse event without disproportionate consequences (Bruneau et al., 2003). Thus, they contribute to robustness (Agarwal, 2015; Van Wee et al., 2019) and are, by extension, negatively correlated to vulnerability. Previous studies have assessed the vulnerability of single and multimodal transport systems in terms of loss in network performance (from a topological or system-based perspective) that would result from the failure of network infrastructure (Mattsson and Jenelius, 2015). This is achieved by failing one network component at a time to identify those components which are most critical to network performance (Rodríguez-Núñez and García-Palomares, 2014; Cats and Jenelius, 2014). A variant of this approach, known as the cell-space method, has been designed to capture the vulnerability of geographically interdependent networks to spatially-defined events, which involves overlaying the networks with a regular grid of cells and then computing, for each cell in turn, the impact of the failure of all infrastructure within cells (Johansson and Hassel, 2010; Ouyang, 2014). The vulnerability of multimodal transport networks with geographic interdependencies has been also evaluated by linking road and railway networks at points where a motorway bridge crosses the railway network and vice versa (Ferrari and Santagata, 2023).

Whilst transport vulnerability has been comprehensively researched in recent years, these studies often reveal issues stemming from a lack of system redundancy. Therefore, gaining insight into the redundancy (and substitutability) of a system has the potential to shed light on the root cause of these issues and to identify key areas for improvement. Methodologically, vulnerability studies require the development of disruption scenarios with which to test the network whereas redundancy analyses do not require any prior assumption of disruption. Moreover, these scenarios are predominately based on the failure of single links (or adjacent links within defined cells) whereas redundancy focusses on the quality of route options between Origin-Destination (OD) pairs. This route-based approach is particularly pertinent when considering geographical interdependency since higher levels of interdependency reduces the level of redundancy between OD pairs which is not something that would be evident from vulnerability analysis.

This study aims to assess the impact of geographic interdependencies on the redundancy and substitutability of discrete public transport infrastructure networks. This aim is achieved by developing two resilience measures which consider the contributions of each network to accessibility whilst accounting for the spatial proximity between network components. The measures are then applied to the Scottish public transport network consisting of long-distance bus and railway services.

The rest of the paper is organised as follows. Section 2 provides a review of relevant literature and Section 3 includes the research methods. In Section 4 the case study is presented, followed by the results in Section 5. Finally, Section 6 includes conclusions and discussion.

2. Key literature on the redundancy and substitutability of transport networks

In the past decade, the redundancy of transport networks has received growing attention. Xu et al. (2018) proposed two measures capturing the number of connections with realistic travel times between locations and applied these to an urban road network. Similar approaches were developed by Jing et al. (2019) who measured redundancy between each pair of stations in a metro network, and by Yang et al. (2016) who proposed a network-level redundancy index reflecting the average number of routes between all stations of an urban rail network. The metrics discussed above assess redundancy from a topological perspective. Taking a different approach, Liao and van Wee (2017) developed an indicator for the diversity of travel options

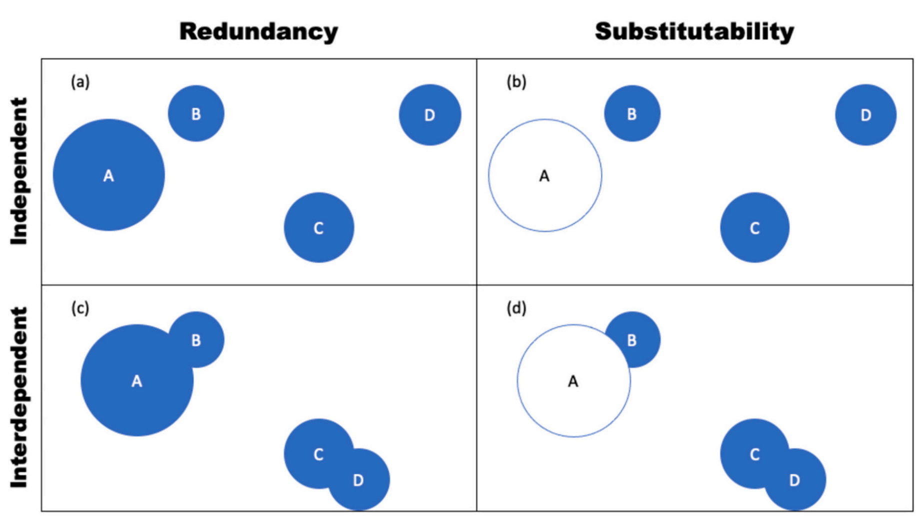

Fig. 1. Comparison of redundancy and substitutability, with and without geographical interdependency. All figures show a choice set containing a total of four options (A-D) which is equal to the unweighted redundancy of options. The size of options indicates the attractiveness of each option; thus, Option A is the preferred option. The intersection of options $A \bigcap B$ plus $C \bigcap D$ is the degree of geographical interdependency in each choice set. In Fig. 1(a) and (c), the sum of weighted options ($A \bigcup B \bigcup C \bigcup D$) is the weighted redundancy which is equivalent to the accessibility presented by the options. In Fig. 1(b) and (d), Option A is unavailable, thus the remaining accessibility is equal to $(((A' \cap B) \bigcup (C \bigcup D))$ which is the substitutability of each choice set.

considering each option's travel time and the extent of overlap between options, and subsequently applied it to a regional multimodal network. Mamun et al. (2013) measured the redundancy of bus travel options between census zones by developing and applying an index that considered the number of available routes and their associated travel times. Li et al. (2024) proposed route diversity measures reflecting the number of routes between origin-destination pairs, their corresponding travel costs and the level of overlap between them, and subsequently used these to evaluate the redundancy offered by urban multimodal bus and metro networks.

In contrast, limited work has been undertaken on substitutability within the context of resilience. Van Wee et al. (2019) defined substitutability as the reduction in accessibility occurring when the preferred option becomes unavailable. Building on this idea, Bondemark et al. (2021) measured substitutability between transport modes as the reduction in accessibility of locations, when a mode becomes unavailable. Chan et al. (2023) developed a metric that captures available options based on their travel time and monetary cost, and further examined how unappealing alternatives could be adjusted to improve spatial equity of options, thus providing insights into how substitutability of options can be enhanced. Another body of research has explored substitutability between travel modes from an impact-based perspective. For example, Ouyang et al. (2015) measured the extent to which rail can substitute the airline network of China when the latter experiences disruptions, by comparing the accessibilities of locations offered by the airline network with and without considering the substitute rail services. Taking a similar approach, Hong et al. (2017) examined how well the urban bus and subway networks can substitute for each other, when one of them is disrupted. Although still in its infancy, current research shows that, by focusing on the attractiveness of options, substitutability provides further insights into the characteristics of resilience of networks, and how well alternative options can replace a preferred one.

These substitutability measures pertain to events affecting only one option at a time and cannot be applied directly to the situation when area-wide events concurrently disrupt more than one modal option. While geographic interdependencies have been explored between transport and other networks (e.g., Dong et al., 2020; Li et al. (2019); Pant et al., 2016; Patterson and Apostolakis, 2007; Zorn et al., 2020), no study has assessed this interdependency between transport modes which use discrete infrastructure networks.

3. Methods

3.1. Network representation

Each public transport network is represented by a graph G consisting of a set of nodes $N = \{n_1, n_2, \ldots, n_K\}$ and a set of segments $E = \{e_1, e_2, \ldots, e_M\}$, where K is the number of nodes and M is the number of segments. Each node corresponds to a public transport stop and each segment represents the transport infrastructure connecting two nodes (e.g., railway tracks, roads) consecutively serviced by a public transport trip. The segment is characterised by a shape, which is dictated by the travel paths that public transport vehicles take along the infrastructure. A set of trips, denoted by $L = \{l_1, l_2, \ldots, l_S\}$ operates on each segment, where S is the total number of trips. Each trip is associated with a schedule defined by a sequence of nodes. Thus a trip l is expressed as $l = \{n_{lO}, n_{l1}, n_{l2}, \ldots, n_{lT}\}$, where n_{lO} is the origin station and n_{lT} is the terminal station of the trip.

In the following sections indicators of redundancy and substitutability are proposed which reflect the potential for concurrent disruption to alternative routes from spatially-defined events. These indicators are extensions of previous work which adjusted redundancy or substitutability on the basis of the shared use of infrastructure as discussed above. Here, the adjustment reflects the extent to which alternative routes fall within a specified distance of each other and thus would be exposed to the impact of the same event.

Redundancy can be viewed as the total accessibility offered by alternative routes minus the contribution to accessibility from spatially proximate infrastructure. Similarly, substitutability can be viewed as the total accessibility minus the accessibility offered by the preferred route and the contribution to the remaining accessibility from spatially proximate infrastructure.

3.2. Redundancy Indicator

The following redundancy indicator is based on an indicator of "robustness"[1] proposed by Liao and van Wee (2017) which is adapted in this paper to consider the degree of geographic interdependency between two networks by introducing a term based on spatial proximity.

When considering a single mode m_1, let p_{m_1} denote the least-cost route connecting an origin-destination pair, OD. The accessibility offered by m_1 is expressed in Eq. (1) (Liao and van Wee, 2017). The negative exponential form is derived from the widely used gravity-based measure, based on which higher costs of options result in lower accessibility values (Geurs and Van Wee, 2004).

$$acc_{OD}^{m_1} = exp\left(-\frac{C(p_{m_1})}{\beta_{m_1}}\right) \tag{1}$$

Where $C(p_{m_1})$ represents the cost of travel along p_{m_1} and β_{m_1} indicates the maximum travel cost acceptable to travellers. If the indicator refers to the same region and the same types of destinations, then β_{m_1} can be set arbitrarily as all indicator values are corrected equally (Liao and van Wee, 2017).

Now consider that mode m_2 is an alternative to m_1. Following Liao and van Wee (2017), the measure in Eq. (1) can be extended by adding the accessibility offered by m_2, $acc_{OD}^{m_2}$. When routes p_{m_1} and p_{m_2} are not spatially proximate to each other, and, thus, not subject to geographic independencies, the contribution of m_2 to the overall level of accessibility is $acc_{OD}^{m_2}$ and hence the redundancy between OD is the sum of $acc_{OD}^{m_1}$ and $acc_{OD}^{m_2}$, as shown in Eq. (2) below. This extended measure reflects the degree of redundancy offered by the two modes.

$$acc_{OD}^{m_1 \leftarrow m_2} = acc_{OD}^{m_1} + acc_{OD}^{m_2} \tag{2}$$

However, in case that p_{m_2} is in the vicinity of p_{m_1}, a correction factor is introduced to account for the geographic interdependency between m_1 and m_2. This factor is referred to as the neighbourhood coefficient and denotes the share of length of p_{m_2} which lies within a specified distance of p_{m_1}. This formulation is presented in Eq. (3). The reduced contribution of m_2 to the accessibility of OD via m_1, due to the proximity between the routes is included in Eq. (4).

$$R_C(p_{m_2}, p_{m_1}) = l(p_{m_2}, p_{m_1}) / l(p_{m_2}) \tag{3}$$

$$acc_{OD}^{m_1 \leftarrow m_2} = exp\left(-\frac{C(p_{m_1})}{\beta_{m_1}}\right) + exp\left(-\frac{C(p_{m_2})}{\beta_{m_2}}\right) \bullet \left[1 - R_C(p_{m_2}, p_{m_1})\right] \tag{4}$$

where $R_C(p_{m_2}, p_{m_1})$ is the neighbourhood coefficient, $l(p_{m_2})$ is the length of p_{m_2}, and $l(p_{m_2}, p_{m_1})$ is the length of p_{m_2} in the neighbourhood of p_{m_1}.

The neighbourhood of routes was represented by buffer zones constructed around them. Fig. 2 illustrates an example of p_{m_2} lying partially in the neighbourhood of p_{m_1}.

Eq. (4) includes the positive effects of the alternative mode m_2 to the

[1] Because in their work, robustness was perceived as the number of travel options available between an origin-destination pair, we argue that redundancy is a more pertinent term; hence, the adapted indicator will be referred to as redundancy indicator.

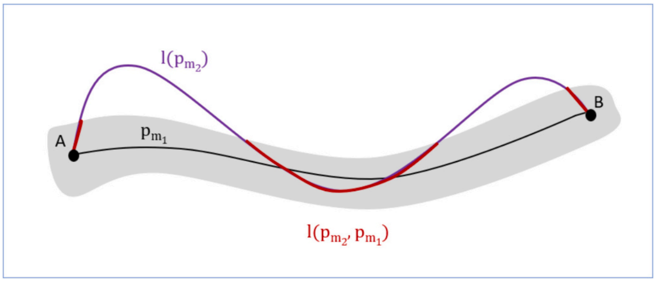

Fig. 2. Example of a route of the alternative transport mode (purple line) located in the buffer-based neighbourhood (grey area) of the primary route (red line). (For interpretation of the references to colour in this figure legend, the reader is referred to the web version of this article.)

primary mode m_1 in connecting a pair of locations, whilst considering geographic interdependencies.

Similarly, $acc_{OD}^{m_2 \leftarrow m_1}$ reflects the redundancy offered by m_2 and m_1, when taking into account the spatial proximity of the two routes. These two indicators are not necessarily equal, because the share of length of p_{m_2} in the neighbourhood of p_{m_1} is not equal to the share of length of p_{m_1} in the neighbourhood of p_{m_2}, and therefore both indicators were computed. For example, for a pair of locations where accessibilities acc^{m_1} and acc^{m_2} are approximately equal, if the share of p_{m_2} in the neighbourhood of p_{m_1} is lower than the share of p_{m_1} in the neighbourhood of p_{m_2}, i.e., $R_c(p_{m_2}, p_{m_1})$ is lower than $R_c(p_{m_1}, p_{m_2})$, then the redundancy $acc^{m_1 \leftarrow m_2}$ will be higher than $acc^{m_2 \leftarrow m_1}$. This in turn indicates that using m_1 as the primary mode of travel and m_2 as alternative provides more resilient connectivity between the pair of locations than when m_2 is the primary mode.

If p_{m_2} is entirely within the neighbourhood of p_{m_1}, then $R_c(p_{m_2}, p_{m_1})$ takes the value of 1, and therefore $acc_{OD}^{m_1 \leftarrow m_2, y=1}$ takes its minimum value given by Eq. (1), while if p_{m_2} is entirely outside of the neighbourhood of p_{m_1}, then $R_c(p_{m_2}, p_{m_1})$ is zero and, as such, $acc_{OD}^{m_1 \leftarrow m_2, y=1}$ takes its maximum value (Eq. (2)).

The redundancy indicator can be aggregated by origin i or destination j, as shown in Eqs. (5) and (6) respectively, to assess the redundancy of travel options from each origin to all zones (Eq. (5)) or from all zones to each destination (Eq. (6)).

$$Acc_i^{(m_1 \leftarrow m_2)} = \sum_{j=1}^{N} \left(acc_{ij}^{m_1 \leftarrow m_2} \right) \tag{5}$$

$$Acc_j^{(m_1 \leftarrow m_2)} = \sum_{i=1}^{M} \left(acc_{ij}^{m_1 \leftarrow m_2} \right) \tag{6}$$

where $j = \{1, 2, \dots N\}$ is the set of destinations and $i = \{1, 2, \dots M\}$ is the set of origins.

For this study, the redundancy indicator was used to determine the loss in redundancy because of area-wide events concurrently affecting two modes m_1 and m_2.

The opportunities available at the destination zones were not considered, as the scope of this work focuses on the impacts of geographic interdependency on the connectivity offered by two discrete networks, rather than the wider implications on the activity system.

In the absence of empirical data, it was assumed that both β_{m_1} and β_{m_2} were equal to 12 h which was considered as the maximum travel time that users of both m_1 and m_2 are willing to travel. In reality these coefficients may not be equal because users may place different limits on the maximum time they would be willing to spend on different modes, for example due to variations in the levels of comfort provided.

The redundancy indicator was computed as follows:

Case I. The positive effects of m_2 were added to the level of accessibility, without accounting for geographic interdependencies between m_1 and m_2.

For each OD pair, the neighbourhood coefficient was zero, and therefore $acc_{ij}^{(m_1 \leftarrow m_2)\boldsymbol{I}}$ was estimated from Eq. (2). The redundancy indicator was computed for each origin zone, $Acc_i^{(m_1 \leftarrow m_2)\boldsymbol{I}}$ using Eq. (5).

Case II. The positive effects of m_2 were added to the level of accessibility, accounting for geographic interdependencies between m_1 and m_2.

For each OD pair, the redundancy $acc_{ij}^{(m_1 \leftarrow m_2)\boldsymbol{II}}$ was quantified using Eq. (4). The value of neighbourhood coefficient was computed using Eq. (3). The redundancy indicator was again computed for each origin zone, $Acc_i^{(m_1 \leftarrow m_2)\boldsymbol{II}}$ from Eq. (5).

The losses in redundancy for each origin because of geographic interdependencies were computed using Eqs. (7) and (8) below.

$$\Delta Acc_{s,m_1}^{(ab)} = Acc_s^{(m_1 \leftarrow m_2)\boldsymbol{II}} - Acc_s^{(m_1)\boldsymbol{I}} \tag{7}$$

$$\Delta Acc_{s,m_1}^{(rel)} = \left(Acc_s^{(m_1 \leftarrow m_2)\boldsymbol{II}} - Acc_s^{(m_1)\boldsymbol{I}} \right) \Big/ A_s^{(m_1)\boldsymbol{I}} \tag{8}$$

3.3. Substitutability indicator

The model of substitutability developed by Van Wee et al. (2019) was adapted to incorporate geographic interdependencies between two modes. Van Wee et al. (2019) defined substitutability as the change in accessibility when the least-cost option is unavailable (Eq. (9)). The normalised substitutability, which ranges between 0 and 1, is shown in Eq. (10). When the normalised measure is close to 0, the substitutability between the OD pair is very poor, whilst when the value is 1, the preferred option can be fully substituted by alternatives without any accessibility loss.

$$S_{OD} = \frac{1}{LS_{OD} - LS_{OD}^{Y=i}} \tag{9}$$

$$\widehat{S}_{OD} = 1 - \frac{1}{1 + S_{OD}} \tag{10}$$

where S_{OD} is the degree of substitutability for an OD pair and $\widehat{S}_{OD}$ is the normalised substitutability measure. LS_{OD} is the total accessibility (i.e. the maximum expected utility) of all options between OD under normal conditions and $LS_{OD}^{Y=i}$ is the accessibility of remaining options when the preferred choice i is unavailable.

Although Eqs. (9) and (10) remain unchanged, the remaining utility was adapted to incorporate the geographic interdependency between m_1 and m_2. When both p_{m_1} and p_{m_2} are available, where the former is the preferred option and the latter is the alternative, their maximum utility, $LS_{OD}^{m_1 \leftarrow m_2}$, is as shown in Eq. (11). When p_{m_1} becomes unavailable and the two routes are distant from each other, and thus there are no geographic interdependencies, the remaining utility $LS_{OD}^{m_1 \leftarrow m_2, y=1}$ is given in Eq. (12).

$$LS_{OD}^{m_1 \leftarrow m_2} = ln\left(acc_{OD}^{m_1} + acc_{OD}^{m_2} \right) \tag{11}$$

$$LS_{OD}^{m_1 \leftarrow m_2, y=1} = ln\left(acc_{OD}^{m_2} \right) \tag{12}$$

where $acc_{OD}^{m_1}$ and $acc_{OD}^{m_2}$ can be computed using Eq. (1).

However, when p_{m_2} is in the vicinity of p_{m_1}, the neighbourhood coefficient of Eq. (3) is introduced to reflect the potential for that part of p_{m_2} which lies in the neighbourhood of p_{m_1}, to be concurrently disrupted. The remaining utility in this case is shown in Eq. (13).

$$LS_{OD}^{m_1 \leftarrow m_2, y=1} = ln\left(acc_{OD}^{m_2} \bullet \left[1 - R_c(p_{m_2}, p_{m_1}) \right] \right) \tag{13}$$

In case that p_{m_2} is entirely within the neighbourhood of p_{m_1}, and thus $R_c(p_{m_2}, p_{m_1})$ is one, the remaining utility of Eq. (13) approaches negative infinity and, therefore, substitutability is zero.

Similarly with redundancy, the normalised substitutability indicator was obtained for origins, without accounting for geographic interdependencies between the two modes (Case I) and when accounting for them (Case II). In the former case, the neighbourhood coefficient of substitute routes was set to zero, while in the latter case it was computed using Eq. (3). Consequently, the absolute and relative losses in substitutability for the origins were computed in a similar way to the indicator of redundancy.

4. Application to rail and long-distance bus networks in mainland Scotland

The services provided by the public transport system range from local, operating mainly in urban areas (e.g., local bus, subway), to regional and long-distance services, which provide connectivity between cities and regions (e.g., certain railway, long-distance bus/coach services). Because the focus of this work is on services that can act as alternatives to each other, modes operating on the same functional scale were selected. Thus, discrete public transport networks for long-distance travel consisting of railway and coach/bus services in mainland Scotland were used to illustrate the application of measures described in Section 3.

The main data sources for the networks were the publicly-available General Transit Feed Specification (GTFS) data for railway (Association of Train Operating Companies, 2020) and bus (Traveline, 2019). For each mode, the data contains information on the stops, routes, trips and timetable of services of the relevant operating companies. The GTFS datasets were initially filtered based on the rail stations and bus stops located within the mainland of Scotland. Contrary to the rail dataset that

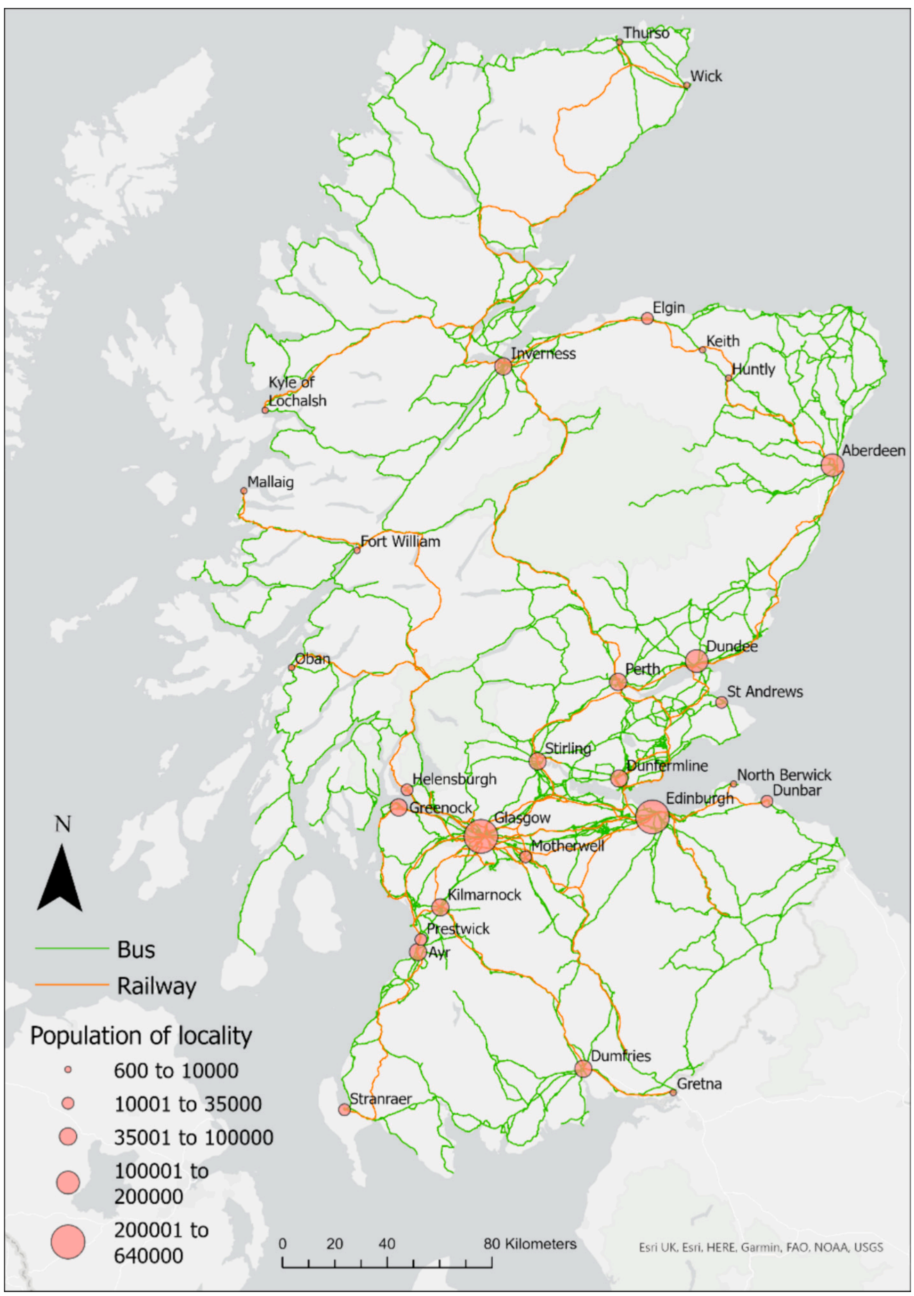

Fig. 3. Travel paths of the long-distance public transport network in mainland Scotland, along with selected Scottish cities and towns and their respective population.

relates to regional and long-distance routes exclusively, the available dataset for bus made no distinction between urban and long-distance services (i.e. all bus routes were recorded as belonging to the same route type) and, therefore, it was not possible to directly extract data associated exclusively with long-distance bus travel. While most long-distance services in Scotland are operated by certain companies, such as National Express, Stagecoach and Megabus, there are multiple operators for urban travel that also provide longer-distance services. Therefore, with a view to retaining only long-distance bus routes, the length of bus routes was used to characterise long-distance travel. Because there is no consensus on how long-distance travel is defined (Aultman-Hall, 2018), with thresholds ranging between 24 km in the UK (van de Velde, 2013) and over 80 km in the United States (Outwater et al., 2015), a 30 km threshold was selected in this study which removed bus routes within urban areas and also between adjacent urban areas from the final dataset. OpenTripPlanner (OTP) (OpenTripPlanner, 2022) was used to obtain travel distances between the termini, and only those routes longer than 30 km long were retained.

The GTFS data was then related to spatially accurate models of the railway and bus infrastructure networks. For bus, the OS MasterMap Highways Network (Ordnance Survey (GB), 2021) was used and, for railway, a model was created using spatial data on railway lines and junctions provided by Network Rail (Network Rail, personal communication, 7 June 2021). In each case, routes were constructed by finding the shortest path between consecutive stops/stations for each unique service contained in the GTFS data. The final representation of these two discrete public transport networks is shown in Fig. 3.

To measure accessibility between locations, a grid was formed dividing the study area into cells representing travel zones. A hexagonal grid was selected because it is preferred when exploring connectivity (Birch et al., 2007). Using the same reasoning as that for the identification of long-distance bus routes, the cell size was selected to have a 30 km long diagonal to exclude short trips. Proximity analysis between localities (cities and towns in Scotland with population of more than 500) revealed that only 8% of locality pairs were related to separation distances of less than 30 km. These are adjacent localities (e.g., Prestwick to Ayr) forming parts of the same continuous urban area and thus travel between them was not considered long-distance. Therefore, it was concluded that the selected cell size was appropriate for this work. For zones partly located outside of Scotland, only the part lying within the country was considered in the analysis. Furthermore, zones separated by un-spanned stretches of coastal water were subdivided to avoid problems in connectivity with the rest of the zoning system. As the focus is on locations serviced by both modes, only zones containing at least one stop of each mode were considered.

OTP was used to estimate the least-cost routes between zones. Two joint public transport-walk networks were constructed, one for each mode, using the street network provided by OpenStreetMap (OpenStreetMap, 2022) and relevant GTFS dataset. Owing to the nature of the GTFS data, the models were schedule-based, rather than frequency-based, as they use the actual timetable of services. Subsequently, route analysis was performed between all OD pairs. The day of journeys was set to Monday and potential times of departure were set for a time window between 7:30 am and 9:30 am, the former time being the earliest possible time of departure and the latter being the latest. This time window was selected to be relatively long to avoid excluding from the analysis infrequent rail and bus services that connect rural and remote areas.

Since access to long-distance services can be achieved via various modes, e.g. walking, bus and taxi, the start and end point of travel were taken to be the stops closest to the centroid of origin and destination zones. The maximum walking distance when transferring between services was restricted to 5 km to prohibit excessive walking, and the maximum number of transfers was set to 2 on the assumption that travellers making longer-distance journeys have a higher willingness to transfer between routes than those on shorter journeys.

Then, route analysis was performed between all combinations of candidate stops in the origin and destination zones, and the least-cost route identified across all possible departure times within the two-hour time window was selected on the basis of travel time.

The output itineraries derived from OTP included the start and end journey times, number of transfers, duration of journey, service (or services) used, boarding and alighting stops, and boarding and alighting times for each service. Owing to the travellers' flexibility to start their journey within the defined time window, there was no waiting time at the start of each journey, however the waiting time arising from transfers between services was included. A spatial representation of these itineraries was then constructed by identifying the routes of services used by the traveller and linking them to the spatially accurate travel paths of networks (Fig. 3), to enable geographical proximity between alternative bus and railway routes to be estimated.

5. Results

Based on the travel times of least-cost routes between OD pairs, the accessibility offered by bus and rail routes were calculated using Eq. (1). For simplicity, routes connecting OD pairs served by both modes will be henceforth referred to as alternative routes. Fig. 4 shows the distribution of accessibility values characterising the alternative routes.

Fig. 4 shows that high accessibility values, especially those higher than 0.8, are more prevalent to each mode than low values. Furthermore, the distributions show that travel by rail is associated with slightly higher accessibility than bus which was expected as travel times by train are generally lower than travel times by bus.

To assess the geographic distribution of accessibility offered by rail and bus jointly, accessibility values of routes were aggregated for origins and destinations (Eqs. (5) and (6)), as shown in Fig. 5.

Fig. 5 reveals significant similarities in the accessibility for travel from origins and to destinations. In both cases, a cluster of high accessibility is observed in the central part of Scotland ("Central Belt"), where the largest and most populated cities are located, such as Glasgow and Edinburgh. Zones containing less populated localities in North Scotland (e.g., Oban, Mallaig, Inverness) and South Scotland (e.g., Ayr, Stranraer, Dumfries), but also in the area above the Central Belt are associated with lower accessibility values. Finally, other zones where smaller settlements are located (e.g., Elgin, Thurso, Wick) are related to the lowest accessibility values.

5.1. *Redundancy of options accounting for geographic interdependencies between modes*

To assess how the positive effects of redundancy diminish due to potential geographic interdependencies, the redundancy indicator (Eq. (4)) was computed for various buffer widths and the losses in redundancy due to geographic interdependencies were obtained (Fig. 6).

Fig. 6 reveals that, as expected, for hazards with a 100 m footprint, the redundancy of OD pairs exhibits slight losses, and as the buffer widths increase, the losses continue to increase gradually. For the most localised hazard, the relative losses for most OD pairs are less than 15%, which indicates that only a small part of the alternative route is within the 100 m-wide buffer of the primary route and, thus, the contribution of former to the redundancy is reduced only by a small percentage. On the other hand, for the most large-scale hazard, losses can be as much as 60%, revealing that a significant part of the substitute route is in the 10 km-wide buffer of the primary, consequently reducing markedly the contribution of substitute mode to the redundancy. Post-hoc comparisons of redundancy values were performed between the case where proximity is ignored and all other cases using Dunn's test (Table S1) which revealed that the losses are statistically significant in all cases, indicating that, regardless of their spatial extent, hazards markedly influence redundancy of travel options.

For small buffer widths, the outliers of Fig. 6 represent location pairs

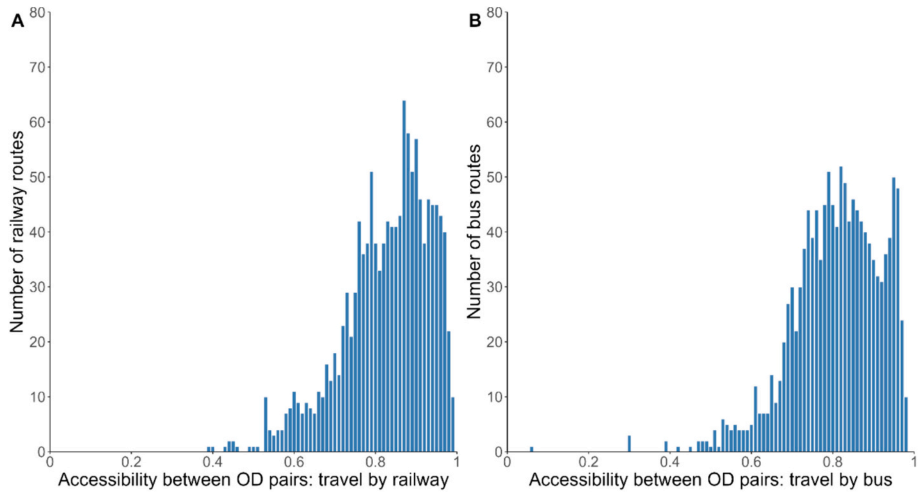

Fig. 4. Histograms of accessibility for the (A) railway and (B) bus routes for OD pairs served by both modes on Monday between 07:30 am and 09:30 am. Accessibility values for a particular mode range from approximately 0 to 1. Low values of accessibility indicate long travel times close to 12 h, while high accessibility values indicate short travel times.

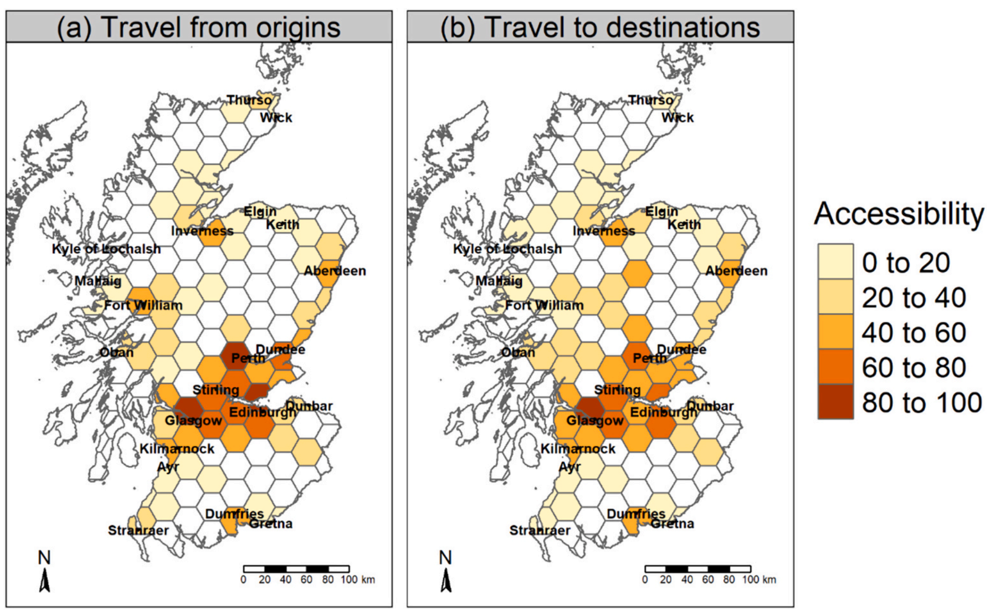

Fig. 5. Maps showing accessibility-based redundancy values of zones connected by both modes for (a) travel from origins (b) travel to destinations, when ignoring geographic interdependencies between the two networks. Non-shaded zones are those not served by both modes. Zones in lighter colours are characterised by lower accessibility than those in darker colours.

related to particularly high redundancy losses and thus particularly susceptible to geographic interdependencies. The OD pairs related to outliers for 100 m-wide buffers, along with the sections of routes that contribute to this susceptibility, are shown in Fig. 7.

The results reveal that the most susceptible OD pairs are similar for rail and bus (Fig. 7(a) and Fig. 7(b)). It is observed that these pairs of locations share the same region, particularly the northern part of the country, while a few OD pairs are also scattered in the rest of the country. Sections of routes that contribute to these high losses are identified in Fig. 7(c) and Fig. 7(d). Most of these sections are located in North Scotland and are located in very close proximity to each other, thus revealing that even the most localised events may concurrently disrupt these alternative rail and bus routes and result in high accessibility losses.

Finally, the redundancy indicator was aggregated by origin to ascertain the geographic distribution of potential redundancy loss due to geographic interdependencies, shown in Fig. 8. Based on the mean relative losses in redundancy between OD pairs due to geographic interdependencies (Table S1), the buffer widths of 100 m, 1.5 km and 10 km were selected for the zone-level aggregation.

Fig. 8 reveals that, for the 100 m hazard footprint, all zones experience low absolute losses in redundancy (Fig. 8(a)), and only two origins suffer slightly higher relative losses (Fig. 8(d)). For the 1.5 km footprint, absolute losses in redundancy increase for densely-populated zones in Central Belt (Fig. 8(b)). For the rest of Scotland, while absolute losses remain low, they are high in relative terms (Fig. 8(e)), ranging for most zones between 13% and 26%, but also 26% to 39% in some cases. This indicates that as the hazard footprint increases, zones may lose a relatively large percentage of their initial redundancy due to alternative routes connecting them being concurrently disrupted. Finally, for the 10 km footprint, absolute losses are very high in Central Belt, and considerably lower in the rest of the country (Fig. 8(c)). However, when

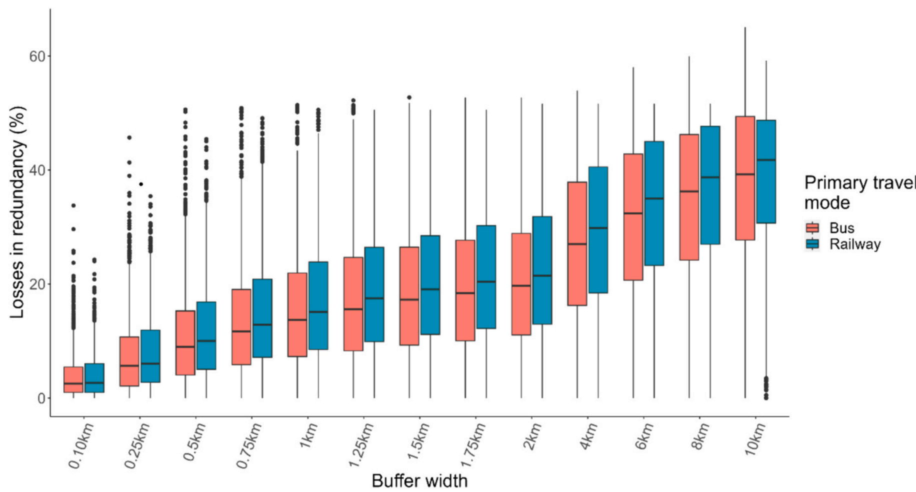

Fig. 6. Relative losses in redundancy of OD Pairs when considering geographic interdependencies related to various neighbourhood sizes. Larger values indicate higher susceptibility of travel options between an OD pair to accessibility loss due to geographic interdependencies, while lower values indicate lower susceptibility.

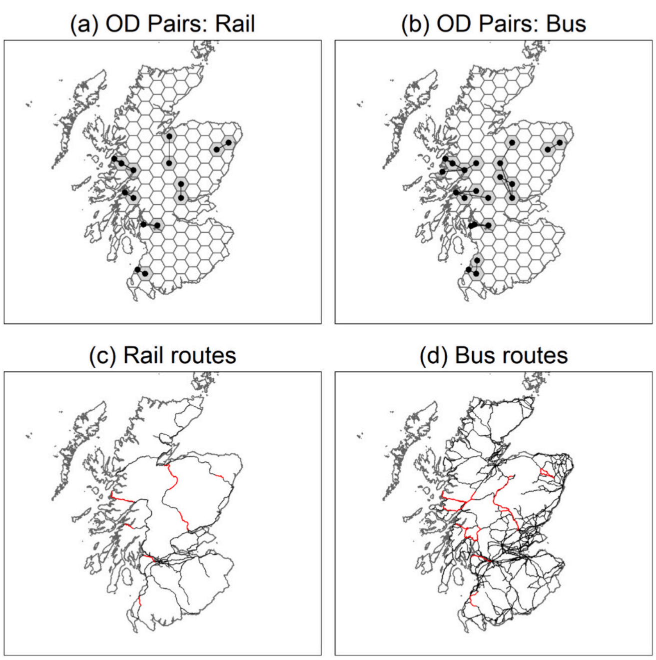

Fig. 7. OD Pairs associated with particularly high redundancy losses where primary mode is (a) rail and (b) bus in the case of 100-m wide buffers, along with sections of (c) rail and (d) bus (road) networks (in red) used by routes connecting these OD pairs. (For interpretation of the references to colour in this figure legend, the reader is referred to the web version of this article.)

considering these in relative terms (Fig. 8(f)), less populated zones outside of Central Belt are the most susceptible to losses arising from geographic interdependencies. Generally, it is observed that relative losses due to large-scale hazards result in significantly high losses across the entire country and especially in less populated zones, revealing that in many cases those zones may lose larger percentage of their initial accessibility than urban zones, when the correlated risk of alternative routes being concurrently disrupted is considered.

Fig. S1 shows the loss in redundancy for origins due to geographic interdependencies when bus is the primary mode and rail is substitute, and the results are very similar to those of Fig. 8.

5.2. Substitutability of options accounting for geographic interdependencies between modes

Fig. 9 shows the distributions of normalised substitutability losses for alternative routes for various buffer widths.

As with redundancy, the box plots of Fig. 9 reveal that losses in substitutability of OD pairs exhibit an upward trend as the buffer widths around primary routes increase. Post-hoc comparisons using Dunn's test (Table S2) showed that geographic interdependencies result in significantly different substitutability values, even for the smallest-scale hazards considered.

As with the redundancy indicator, the routes associated with the high outliers of substitutability losses in the case of 100 m-wide buffers were identified, as shown in Fig. 11, along with the section of public transport routes that contribute to these losses. The results reveal that the OD pairs related to these outliers are in similar locations to those of redundancy (Fig. 7), however they appear to be significantly more, when considering either mode as primary. This shows that while significant discrepancies in the redundancy and substitutability losses do not exist, it further reinforces the observation that it is possible for an OD pair to experience very high losses in substitutability but not in redundancy. Thus, for an OD pair where the primary route is characterised as high accessibility and the alternative route is entirely within the neighbourhood of the former, the redundancy indicator will still be high, while substitutability will be zero.

Regarding the sections of the rail and bus networks that contribute to these high losses in substitutability, Fig. 10(c) and Fig. 10(d) show that these are the same as those for redundancy (Fig. 7), thus revealing that regardless an OD pair is characterised by extremely high losses in redundancy, substitutability (or both), its corresponding routes use specific parts of the network that contribute to its susceptibility to geographic interdependencies.

The normalised substitutability of routes was aggregated for origins for the 100 m, 1.5 km and 10 km footprints, as shown in Fig. 11.

The results for localised hazards (Fig. 11(a) and Fig. 11(d)) suggest that all zones exhibit very low losses in substitutability, which is consistent with those of redundancy (Fig. 8(a) and Fig. 8(d)). However, as the scale of hazard increases, differences between the two indicator values are revealed. While the geographic distribution of absolute losses in redundancy for the 1.5 km-wide buffers (Fig. 8(b)) shares significant similarities with that of normalised substitutability (Fig. 11(b)), the distributions of relative losses exhibit differences as Fig. 11(e) indicates that fewer zones are related to high substitutability losses due to geographic interdependencies than Fig. 8(e). These differences are even

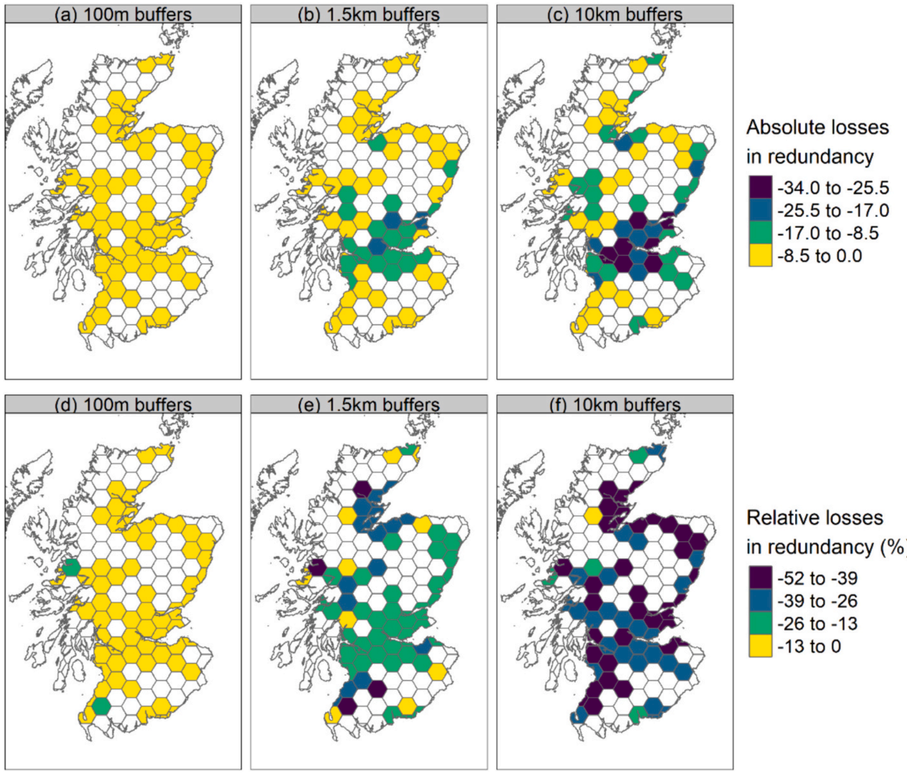

Fig. 8. Losses in redundancy for origins (a) in absolute terms due to hazards of 100 m footprint (b) in absolute terms due to hazards of 1.5 km footprint (c) in absolute terms due to hazards of 10 km footprint (d) in relative terms due to hazards of 100 m footprint (e) in relative terms due to hazards of 1.5 km footprint, and (f) in relative terms due to hazards of 10 km footprint, when rail is considered as primary travel mode and bus as alternative. Non-shaded zones are those origins not served by both modes. Zones in lighter colours are less susceptible to losses due to geographic interdependencies.

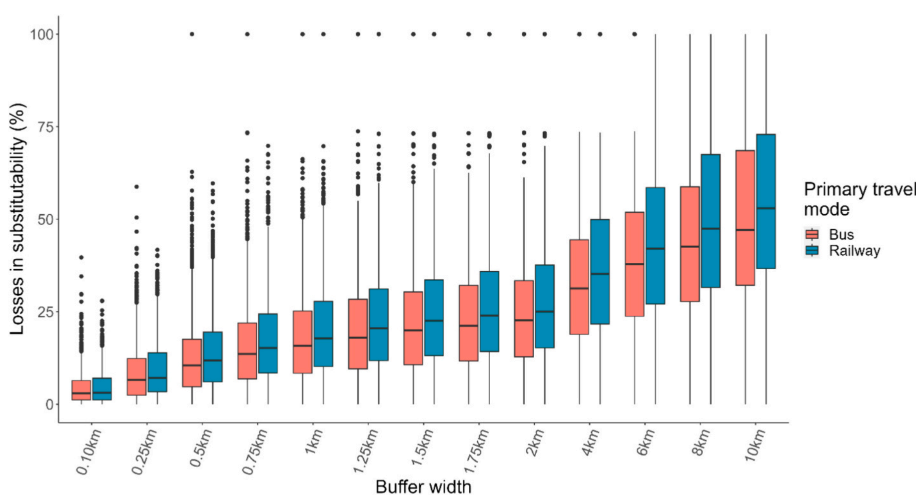

Fig. 9. Losses in normalised substitutability values of alternative routes of each mode for buffers of varying widths. The box plots for bus (orange colour) show substitutability losses when bus is the primary mode and railway is substitute and express the reduction in the extent to which railway routes replace the corresponding bus routes when the latter become unavailable. Likewise, box plots for railway (green colour) reflect the drop in extent to which bus routes replace the accessibility provided by railway routes. (For interpretation of the references to colour in this figure legend, the reader is referred to the web version of this article.)

more significant for the 10 km-wide buffers (Fig. 11(f)) and Fig. 8(f)). This indicates that while a zone may experience very high losses in terms of redundancy, its losses in terms of substitutability may be lower. It is further worth noting that zones that rank high in substitutability losses but low in redundancy are not observed, indicating that using the redundancy indicator to assess losses in accessibility of locations provides more conservative results than the substitutability indicator.

The origin-level losses in substitutability were also computed (Fig. S2) when considering bus as primary mode and reveal very similar results to those of Fig. 11.

6. Conclusions and discussion

In this paper, an approach is presented to assess the role of geographic interdependencies between two discrete public transport networks for two components of resilience, namely redundancy and

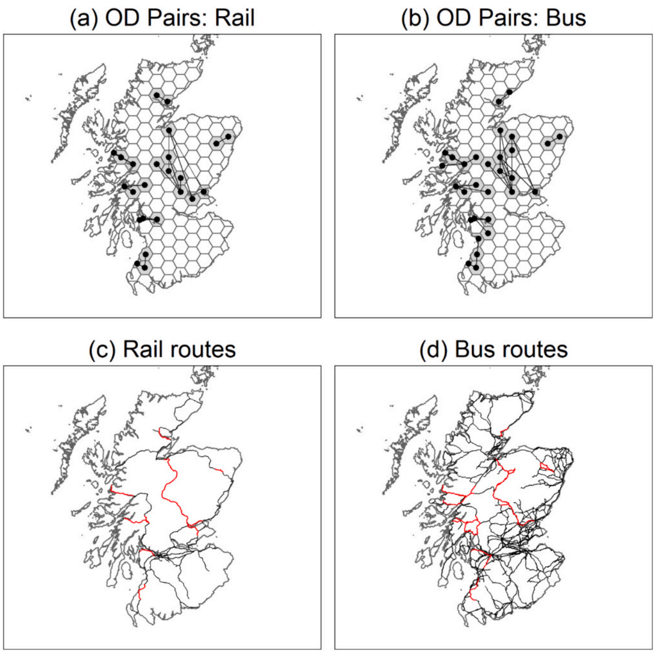

Fig. 10. OD Pairs associated with high outliers of substitutability losses for travel by (a) rail and (b) bus, in the case of 100 m-wide buffers, along with sections of (c) rail and (d) bus (road) networks that the routes connecting these OD Pairs use.

substitutability of travel options. Measures were developed to represent each of these components using an accessibility-based approach. The degree of geographic interdependencies was introduced by reducing the contributions of total accessibility of alternative routes based on the proximity between them. The results reveal that while an alternative mode provides significant resilience benefits, its contributions are potentially reduced when geographic interdependency is considered. The extent of this reduction depends on the spatial footprint of hazards and the degree of proximity of alternative routes, highlighting the importance of careful selection of buffer size. A very small value will result in narrow buffers that underestimate the risk of routes being concurrently disrupted by large-scale events, while wide buffers could overestimate the risk of concurrent disruptions caused by localised events. In the example presented, the redundancy and substitutability of most routes between OD pairs were not significantly affected by small-scale events, however losses became significantly more noticeable for larger-scale hazards.

Furthermore, the results of the example show that, although urban, densely-populated areas are associated with the highest redundancy and substitutability losses in absolute terms, rural areas that are less densely populated lose a higher percentage of their initial values as a result of area-wide events. This is because, although absolute losses in zones located in less populated areas due to geographic interdependency were low, their initial values in redundancy and substitutability (i.e., when ignoring geographic interdependency) were also low. In contrast, absolute losses due to geographic interdependency in urban zones were high, but their initial values in redundancy and substitutability were also high; therefore, these high absolute losses were only a small proportion of their initial indicator values. An important observation of the results highlighted differences in the ranking of OD pairs and locations in terms of redundancy and substitutability, which is attributed to the fact that the former metric places more emphasis on the contribution of the primary option to the accessibility, while the latter focuses more on the remaining accessibility when the primary option is unavailable. These indicators therefore complement each other when assessing the accessibility of locations, with or without accounting for geographic interdependency.

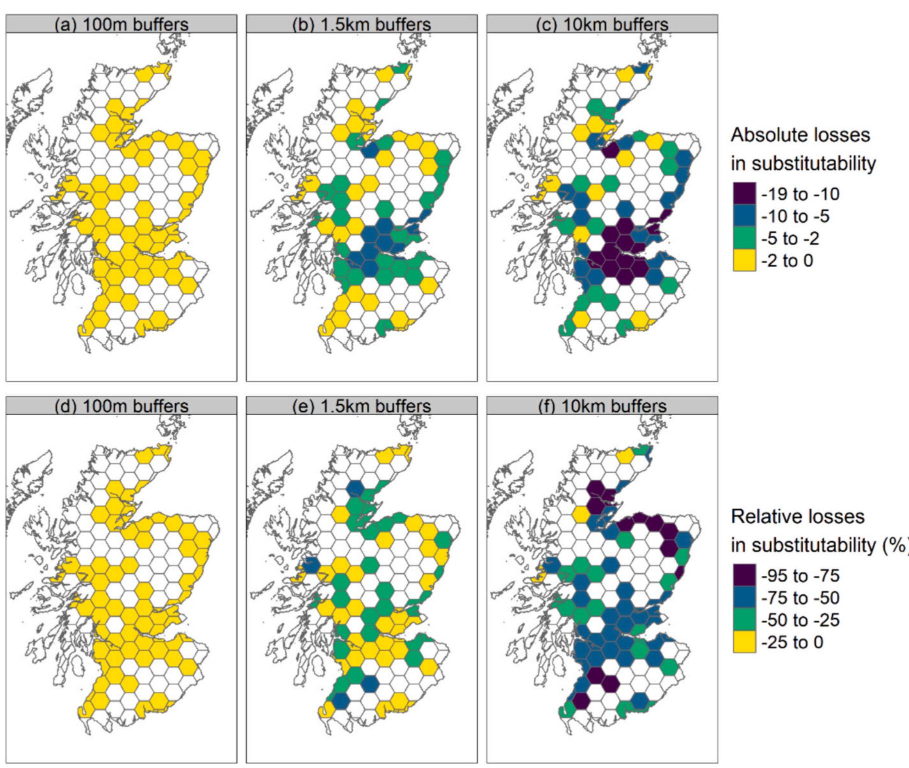

Fig. 11. Losses in normalised substitutability for origins (a) in absolute terms due to hazards of 100 m footprint (b) in absolute terms due to hazards of 1.5 km footprint (c) in absolute terms due to hazards of 10 km footprint (d) in relative terms due to hazards of 100 m footprint (e) in relative terms due to hazards of 1.5 km footprint, and (f) in relative terms due to hazards of 10 km footprint, when rail is considered as primary travel mode and bus as substitute. Non-shaded zones are those origins not served by both modes. Zones in lighter colours are less susceptible to losses due to geographic interdependencies.

The work presented comes with several limitations. Firstly, the redundancy and substitutability measures were assessed in terms of travel time, however other elements of travel deterrence could be considered, such as distance and economic cost of travel. Secondly, for the proposed indicators, rail and bus operating on the same functional level were identified based on the travel distance of their services. However, although the modes selected were largely interchangeable, each has different capacities and flexibilities. For example, typically a bus service may more easily detour in the event of a road closure, while rail can put on replacement buses when trains are disrupted. Thirdly, due to the fact that the available GTFS data for bus services in Scotland made no distinction between local and long-distance routes, the latter were selected based solely on the length of each bus route. This selection could be further refined by retaining bus services with termini in different localities which exceed a given route distance threshold. Another limitation is that the impact of geographic interdependencies on components of resilience was assessed for a certain time-window on a weekday. Choosing a different day or time-of-day may have resulted in different itineraries and, as such, different redundancy and substitutability values. Repeating the analysis for various time-windows (e.g., peak and off-peak times) would allow ascertaining hours-of-day and days-of-week, where resilience of networks is mostly affected by geographic interdependencies.

Furthermore, the geographic interdependencies were estimated using a buffer-based approach where only those parts of alternative routes which lie within the buffer of preferred route were considered, while those parts lying outside of that buffer were ignored. The method could be extended to avoid this “cliff-edge” effect by allowing the degree of geographic interdependency to decay with separation distance between routes. However, capturing the distance-decay effect would be challenging and computationally intensive, as proximity between alternative routes varies along their length. Another limitation of this work is that the potential of two travel options being concurrently disrupted arises purely from their proximity. Whilst horizontal distance is an important determinant for concurrent failures, other factors may influence this, depending on the hazard of concern, such as vertical separation of routes and slope. To better account for these factors, risk maps showing the spatial footprint and intensity of hazards of interest could be used instead of buffers.

Finally, because the focus of this work was to assess the effects of the geographic interdependency between two discrete public transport modes, only the shortest path route of each mode was considered. The method could also include other feasible routes of these modes following the approach of Liao and van Wee (2017), in which the accessibility offered by each additional route is reduced by the extent to which it falls within the buffers of routes which have already been included in the calculation. Likewise, this approach could be extended to include more than two transport modes, as well as the attractiveness of destinations. A general model of redundancy that considers both the value of destination opportunities and the connectivity provided by multiple options is presented in the Supplementary Material.

Despite these limitations, the findings provide novel indications on the impacts of geographic interdependencies related to area-wide events on components of resilience of transport networks. The approach presented enables policy makers and network managers to explore the potential severity of consequences of area-wide events on multimodal transportation networks and identify areas of the network which, if impacted, would lead to the highest losses in accessibility.

Author agreement statement

We declare that this manuscript is original, has not been published before and is not currently being considered for publication elsewhere.

We confirm that the manuscript has been read and approved by all named authors and that there are no other persons who satisfied the criteria for authorship but are not listed. We further confirm that the order of authors listed in the manuscript has been approved by all of us.

Funding

This research did not receive any specific grant from funding agencies in the public, commercial, or not-for-profit sectors.

CRediT authorship contribution statement

Georgia Boura: Writing – original draft, Visualization, Methodology, Investigation, Formal analysis, Data curation, Conceptualization. **Neil S. Ferguson:** Writing – review & editing, Validation, Supervision, Methodology, Conceptualization.

Declaration of competing interest

None.

Data availability

Data will be made available on request.

Acknowledgements

The authors would like to thank the reviewers for their valuable comments and suggestions which helped to improve this paper. The authors would also like to thank Network Rail for providing the spatial data of railway lines and junctions that enabled constructing the spatial representation of the railway network. The following R packages were used, and the authors would like to acknowledge their developers: tmap (Tennekes et al., 2021), sf (Pebesma, 2018), tidyverse (Wickham et al., 2019), ggplot2 (Wickham, 2011), otpr (Young, 2020).

Appendix A. Supplementary data

Supplementary data to this article can be found online at https://doi.org/10.1016/j.jtrangeo.2024.103934.

References

Agarwal, J., 2015. Improving resilience through vulnerability assessment and management. Civ. Eng. Environ. Syst. 32 (1–2), 5–17.

Anas, A., 1983. Discrete choice theory, information theory, and the multinomial logit and gravity models. Transp. Res. B 17, 13–23.

Aultman-Hall, L., 2018. Incorporating long-distance travel into transportation planning in the United States.

Association of Train Operating Companies, 2020. ATOC GTFS [Data set]. https://transitfeeds.com/p/association-of-train-operating-companies/284. Accessed 21/09/2020.

Ben-Akiva, M.E., Lerman, S.R., 1985. Discrete Choice Analysis: Theory and Application to Travel Demand. MIT Press, Cambridge, MA.

Berdica, K., 2002. An introduction to road vulnerability: what has been done, is done and should be done. Transp. Policy 9 (2), 117–127.

Birch, C.P., Oom, S.P., Beecham, J.A., 2007. Rectangular and hexagonal grids used for observation, experiment and simulation in ecology. Ecol. Model. 206 (3–4), 347–359.

Bondemark, A., Kopsch, F., Johansson, E., 2021. Accessibility and uncertainty. J. Transp. Land Use 14 (1), 463–477.

Bruneau, M., Chang, S.E., Eguchi, R.T., Lee, G.C., O'Rourke, T.D., Reinhorn, A.M., Von Winterfeldt, D., 2003. A framework to quantitatively assess and enhance the seismic resilience of communities. Earthquake Spectra 19 (4), 733–752.

Cats, O., Jenelius, E., 2014. Dynamic vulnerability analysis of public transport networks: mitigation effects of real-time information. Netw. Spat. Econ. 14 (3), 435–463.

Chan, H.Y., Xu, Y., Chen, A., Zhou, J., 2023. Choice and equity: a critical analysis of multi-modal public transport services. Transp. Policy 140, 114–127.

Dong, S., Wang, H., Mostafizi, A., Song, X., 2020. A network-of-networks percolation analysis of cascading failures in spatially co-located road-sewer infrastructure networks. Phys. A: Stat. Mechan. Appl. 538, 122971.

Dudenhoeffer, D.D., Permann, M.R., Manic, M., 2006, December. CIMS: a framework for infrastructure interdependency modeling and analysis. In: Proceedings of the 2006 Winter Simulation Conference. IEEE, pp. 478–485.

Fathom Global, 2021. Flood Emergency Report Germany 2021. https://www.fathom.global/wp-content/uploads/2021/12/Flood-Emergency-Report-Germany-2021-1_compressed.pdf.

Ferrari, C., Santagata, M., 2023. Vulnerability and robustness of interdependent transport networks in North-Western Italy. Eur. Transp. Res. Rev. 15 (1), 6.
Frappier, A., Morency, C., Trépanier, M., 2018. Measuring the quality and diversity of transit alternatives. Transp. Policy 61, 51–59.
Geurs, K.T., Van Wee, B., 2004. Accessibility evaluation of land-use and transport strategies: review and research directions. J. Transp. Geogr. 12 (2), 127–140.
Hong, L., Yan, Y., Ouyang, M., Tian, H., He, X., 2017. Vulnerability effects of passengers' intermodal transfer distance preference and subway expansion on complementary urban public transportation systems. Reliab. Eng. Syst. Saf. 158, 58–72.
Jenelius, E., Mattsson, L.G., 2020. Resilience of transport systems. In: Encyclopedia of Transportation.
Jing, W., Xu, X., Pu, Y., 2019. Route redundancy-based network topology measure of metro networks. J. Adv. Transp. 2019.
Johansson, J., Hassel, H., 2010. An approach for modelling interdependent infrastructures in the context of vulnerability analysis. Reliab. Eng. Syst. Saf. 95 (12), 1335–1344. https://doi.org/10.1016/j.ress.2010.06.010.
Kays, H.I., Sadri, A.M., Muraleetharan, K.M., Harvey, P.S., Miller, G.A., 2023. Exploring the interdependencies between transportation and Stormwater networks: the case of Norman, Oklahoma. Transp. Res. Rec. 2678 (5), 491–513.
Lee, H., Calvin, K., Dasgupta, D., Krinner, G., Mukherji, A., Thorne, P., Zommers, Z., 2023. Climate Change 2023: Synthesis Report. Contribution of Working Groups I, II and III to the Sixth Assessment Report of the Intergovernmental Panel on Climate Change. The Australian National University.
Li, T., Rong, L., Yan, K., 2019. Vulnerability analysis and critical area identi fi cation of public transport system : a case of high-speed rail and air transport coupling system in China. Transp. Res. A 127 (June), 55–70. https://doi.org/10.1016/j.tra.2019.07.008.
Li, J.Y., Teng, J., Wang, H., 2024. Measuring route diversity in spatial and spatial-temporal public transport networks. Transp. Policy 146, 42–58.
Liao, F., van Wee, B., 2017. Accessibility measures for robustness of the transport system. Transportation 44 (5), 1213–1233. https://doi.org/10.1007/s11116-016-9701-y.
Mamun, S.A., Lownes, N.E., Osleeb, J.P., Bertolaccini, K., 2013. A method to define public transit opportunity space. J. Transp. Geogr. 28, 144–154.
Mattsson, L.G., Jenelius, E., 2015. Vulnerability and resilience of transport systems - a discussion of recent research. Transp. Res. A Policy Pract. 81, 16–34. https://doi.org/10.1016/j.tra.2015.06.002.
Network Rail, 2020. 'Scotland's Railway Weather Resilience and Climate Change Adaptation Plan' – Version 1 – September 2020. Available at: https://www.networkrail.co.uk/wp-content/uploads/2020/10/Scotlands-Railway-WRCCA-Plan-2020-CP6.pdf.
OpenStreetMap. Scotland-Latest.Osm.Pbf [Data Set]. https://download.geofabrik.de/ (Accessed 22/06/2022).
OpenTripPlanner, 2022. (Version 2.1.0) [Computer software]. https://repo1.maven.org/maven2/org/opentripplanner/otp/2.1.0/. Accessed 22/06/2022.
Ordnance Survey (GB), 2021. OS MasterMap Highways Network [GML3 geospatial data], Scale 1:2500, Tiles: GB, Updated: 1 March 2021, Ordnance Survey (GB), Using: EDINA Digimap Ordnance Survey Service. https://digimap.edina.ac.uk. Downloaded: 2021-06-18 18:34:18.522.
Outwater, M., Bradley, M., Ferdous, N., Trevino, S., Lin, H., 2015. Foundational Knowledge to Support a Long-Distance Passenger Travel Demand Modeling Framework: Implementation Report.
Ouyang, M., 2014. Review on modeling and simulation of interdependent critical infrastructure systems. Reliab. Eng. Syst. Saf. 121, 43–60.
Ouyang, M., Pan, Z., Hong, L., He, Y., 2015. Vulnerability analysis of complementary transportation systems with applications to railway and airline systems in China. Reliab. Eng. Syst. Saf. 142, 248–257.
Pant, R., Hall, J.W., Blainey, S.P., 2016. Vulnerability assessment framework for interdependent critical infrastructures: case-study for Great Britain's rail network. Eur. J. Transp. Infrastruct. Res. 16 (1).
Patterson, S.A., Apostolakis, G.E.Ã., 2007. Identification of critical locations across multiple infrastructures for terrorist actions, 92, 1183–1203. https://doi.org/10.1016/j.ress.2006.08.004.
Pebesma, E.J., 2018. Simple features for R: standardized support for spatial vector data. R J. 10 (1), 439.
Rinaldi, S.M., Peerenboom, J.P., Kelly, T.K., 2001. Identifying, understanding, and analyzing critical infrastructure interdependencies. IEEE Control. Syst. Mag. 21 (6), 11–25. https://doi.org/10.1109/37.969131.
Rodríguez-Núñez, E., García-Palomares, J.C., 2014. Measuring the vulnerability of public transport networks. J. Transp. Geogr. 35, 50–63.
Tennekes, M., Nowosad, J., Gombin, J., Jeworutz, S., Russell, K., Zijdeman, R., Clouse, J., Lovelace, R., Muenchow, J., 2021. Tmap: Thematic Maps. https://cran.r-project.org/web/packages/tmap/index.html.
Thacker, S., Barr, S., Pant, R., Hall, J.W., Alderson, D., 2017. Geographic hotspots of critical national infrastructure. Risk Anal. 37 (12), 2490–2505.
Traveline, 2019. GB Bus services [Data set]. https://transitfeeds.com/p/traveline/1033. Accessed 21/09/2020.
van de Velde, D., 2013. Long-distance coach services in Europe. In: Regulating Transport in Europe. Edward Elgar Publishing, pp. 115–139.
Van Wee, B., Van Cranenburgh, S., Maat, K., 2019. Substitutability as a spatial concept to evaluate travel alternatives. J. Transp. Geogr. 79 (January), 102469 https://doi.org/10.1016/j.jtrangeo.2019.102469.
Wickham, H., 2011. ggplot2. Wiley interdisciplinary reviews: computational statistics, 3 (2), 180–185.
Wickham, H., Averick, M., Bryan, J., Chang, W., McGowan, L.D.A., François, R., Yutani, H., 2019. Welcome to the Tidyverse. J. Open Source Softw. 4 (43), 1686.
Xi, Y., Miller, E.J., Saxe, S., 2018. Exploring the impact of different cut-off times on isochrone measurements of accessibility. Transp. Res. Rec. 2672 (49), 113–124.
Xu, X., Chen, A., Jansuwan, S., Yang, C., Ryu, S., 2018. Transportation network redundancy: complementary measures and computational methods. Transp. Res. B Methodol. 114, 68–85.
Yang, X., Chen, A., Ning, B., Tang, T., 2016. Measuring route diversity for urban rail transit networks: a case study of the Beijing metro network. IEEE Trans. Intell. Transp. Syst. 18 (2), 259–268.
Young, M., 2020. Otpr: an R wrapper for the OpenTripPlanner REST API.
Zimmerman, R., 2004, October. Decision-making and the vulnerability of interdependent critical infrastructure. In: 2004 IEEE International Conference on Systems, Man and Cybernetics (IEEE Cat. No. 04CH37583), Vol. 5. IEEE, pp. 4059–4063.
Zorn, C., Pant, R., Thacker, S., Shamseldin, A.Y., 2020. Evaluating the magnitude and spatial extent of disruptions across interdependent national infrastructure networks. ASCE-ASME J. Risk Uncertain. Eng. Syst. Part B: Mechan. Eng. 6 (2), 020904.